JOURNAL OF MATERIALS SCIENCE 16 (1981) 1769–1775

Mechanics of strength-degrading contact flaws in silicon

B. R. LAWN, D. B. MARSHALL*, P. CHANTIKUL
Department of Applied Physics, School of Physics, University of New South Wales, Kensington, NSW 2033, Australia

The micromechanics of indentation-induced flaws in monocrystalline silicon have been studied in relation to strength determination. In the first part, the evolution of the deformation–fracture pattern during contact with a Vickers pyramid is described. Emphasis is thereby placed on the vital role of the residual component of the elastic–plastic contact field in driving the cracks. In the second part, the response of the cracks in subsequent strength testing is followed. A precursor stage of stable growth is observed prior to attaining a failure configuration, consistent with augmentation of the applied tensile (flexural) loading by the residual contact component. No detectable slow crack growth due to environmental influence is found. Nevertheless, silicon is revealed as a material of extreme susceptibility to brittle fracture, with significant strength degradation from contacts on the microscale. The relevance of this brittleness to the mechanical behaviour of silicon components as a function of fabrication and prospective service conditions is discussed.

1. Introduction

The current growth explosion in the semiconductor device industry and in attendant solar cell technology is a commentary on the intense concentration of electronics research on one particular substance – silicon. It is, therefore, somewhat surprising that the mechanical properties of this remarkable material have received little attention in the scientific literature. For, silicon is one of the most brittle of all materials [1], and the incidence of cracking, even on the microscale, can have serious implications in subsequent component performance. Most directly, an incipient microcrack may lead to component malfunction, or even to total failure, if extraneous stresses reach a level at which unstable growth can occur [2, 3]. In a more subtle way, cracks may significantly modify the electronic response, e.g. via the creation of "surface states" at the newly created fracture interface [4, 5].

The question of how microcracks evolve in silicon is thus of some importance if the mechanics of component degradation are to be understood. In this study a "controlled-flaw" approach, in which a standard Vickers diamond pyramid indenter is used to introduce well-defined deformation–fracture patterns into test surfaces, is adopted. Much attention has recently been devoted to the analysis of these patterns in brittle solids, with the express aim of relating the indentation variables (contact load, characteristic pattern dimensions) to intrinsic material parameters (fracture "toughness") [6–12]. Apart from providing a convenient means of controlling the scale of microcracking, the indentation method offers considerable physical insight into damage processes associated with fabrication procedures (e.g. scribing with a point tool [3]) or in-service stress-raising events (e.g. particle impact [13]). A key feature in the crack evolution is the vital contribution of residual contact stresses to the net driving force, with consequent deleterious effects in the strength characteristics [10–12]. Strength testing of specimens containing indentation flaws

*Present address: Materials and Molecular Research Division, Lawrence Berkeley Laboratories, University of California, Berkeley, 94720, USA.

0022–2461/81/071769–07$02.70/0 © *1981 Chapman and Hall Ltd.*

must accordingly reflect on more than just fracture toughness; the material hardness, which quantifies the irreversible component of the contact field, also enters the description. With proper account of the residual stresses one obtains a powerful tool for investigating a wide spectrum of flaw-sensitive mechanical responses in brittle materials; a survey of such responses in the context of evaluating brittle ceramics for structural applications is given elsewhere [14].

In the following sections the indentation–strength behaviour of monocrystalline silicon is examined in detail. The growth history of the induced flaws is considered in terms of two sequentially applied stress fields: (1) the contact field itself, responsible for generating the actual crack system; and (2) a tensile field produced in flexure, responsible ultimately for taking the crack system to failure. The results serve to highlight the extreme susceptibility of silicon to strength-degrading microfracture under normal conditions of component operation.

2. Radial crack evolution in elastic–plastic indentation field

The basic elements of the damage pattern produced in Vickers indentation are well established. Around the sharp point of the pyramidal contact the indented material deforms irreversibly, thereby creating a residual hardness impression. In silicon and other solids with the diamond structure the contact stresses are of the order of the theoretical cohesive strength, so a high density of strain energy is available for nucleating microcracks. Although the elements of irreversible deformation have been identified in several transmission electron microscopy (TEM) studies [15–19], the role of these elements in the flaw-generation process remains obscure. The observation of intense diffraction contrast in the regions of material immediately surrounding the indentation sites in the thinned TEM foils [18] attests to the existence of a strong residual component in the "elastic–plastic" stress field. Analogous observations about linear surface scratches made with a diamond scribing tool have been reported by others using X-ray topography [20] and infrared (i.r.) photoelasticity [21].

Above some threshold in the contact loading a well-defined crack system suddenly develops from the embryo nuclei within the central deformation zone [22]. This threshold is low, <0.1N, for silicon [23]. Two types of crack form, both in penny-like configuration: (1) "median–radial" cracks [12] (hereafter referred to simply as radial cracks), on the two mutually orthogonal median planes of symmetry defined in each case by the indentation axis and one of the impression diagonals, centred on the contact point (i.e. half-penny cracks); (2) "lateral" cracks, emanating from the base of the deformation zone and spreading laterally outward nearly parallel to the surface. The latter crack type can cause chipping, and is therefore particularly pertinent to the problems of surface wear and erosion; the former type, being more penetrative, bears more strongly on the issue of strength degradation. Since it is the strength behaviour which will be our greater concern here, the radial component will be regarded as the primary crack in the damage pattern.

Silicon is, of course, opaque to light in the visible region of the spectrum, so direct observation of subsurface crack development during the contact cycle is not feasible. A fractographic technique involving examination of the crack surfaces after the event was accordingly used [10]. The specimens were single-crystal slices 1 mm thick with an optical quality surface finish. Although the indentation axis was aligned accurately along the near-[1 1 1] surface normal, no attempt was ultimately made to orientate the impression diagonals along a specific crystallographic direction; preliminary tests showed experimental scatter to mask any systematic anisotropy in the crack pattern.* After indentation in air, each specimen was broken by applying a tensile stress normal to one of the median planes (in three-point bending, as described in Section 3), thereby affording a cross-sectional view of the entire subsurface radial crack system. An example is shown in Fig. 1, with a schematic diagram to illustrate how the observed fracture markings (due mainly to spurious disturbances in the indenter drive) relate to the overall damage pattern. The markings reveal a growth history similar to that previously described for glass [10, 12]: during the loading half-cycle the crack is driven outward, but is constrained somewhat at the surface by a compressive component in the elastic point-

*Diamond-type crystals have a {1 1 1} cleavage tendency, but this tendency is not strong: on a simplistic bond-count basis a maximum variation of $3^{1/2}$ is estimated in the surface energies in going from {1 1 1} to {1 0 0} planes [24].

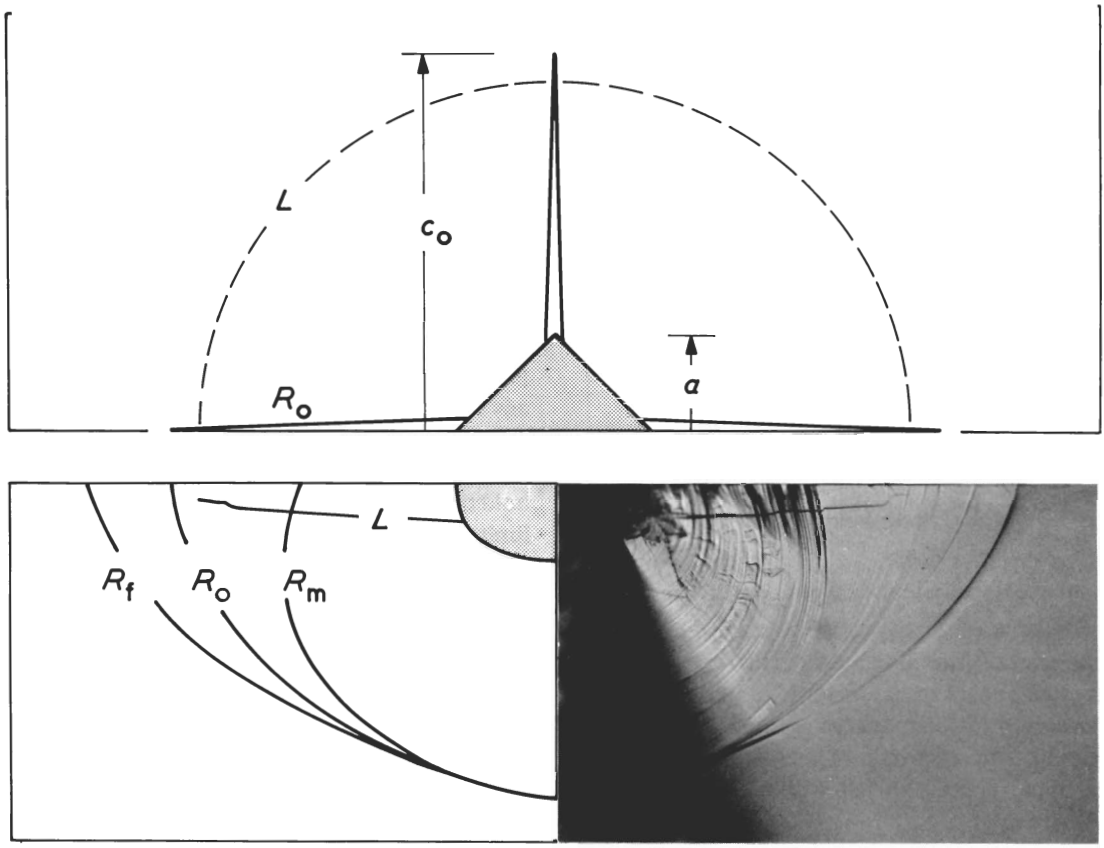

Figure 1 Radial–median crack system in silicon. Micrograph is half-view of crack formed at $P = 30$ N, photographed after fracture on median plane. Schematic diagram at left bottom depicts essential features of fractographic pattern: radial crack front at maximum contact load (R_m), at complete unload (R_o), and at failure in subsequent tensile stressing (R_f); trace of lateral crack (L); deformation zone (shaded). Schematic diagram at the top depicts surface view at complete unload, indicating characteristic dimensions of radial cracks ($c_o = 170\,\mu$m) and deformation impression ($a = 41\,\mu$m).

contact field; during unloading the elastic constraint relaxes, and the radial crack trace continues to extend under the sustained action of the residual stresses generated by elastic–plastic mismatch. In direct contrast to the glass observations, however, the radial cracks showed no tendency to further growth *after* removal of the indenter, suggesting that silicon is not susceptible to atmosphere-enhanced slow crack growth. Surface chipping was also more prevalent in silicon, particularly at higher contact loads, often severely disrupting the surface radial pattern.

Thus the radial crack experiences a persisting driving force which, expressed as a residual stress intensity factor, takes the form [10]

$$K_r = \chi_r P/c_0^{3/2} \qquad (1)$$

where P is the peak contact load, c_0 is the crack length at completion of the contact (Fig. 1), and χ_r is an elastic–plastic constant. Since the surface crack grows stably up to the point of final withdrawal of the indenter, the equilibrium condition $K_r = K_c$ must apply, where K_c defines the material toughness. Hence from Equation 1

$$P/c_0^{3/2} = K_c/\chi_r = \text{constant}. \qquad (2)$$

Fig. 2 shows results obtained from the indentation tests on silicon (the value of c_0 for each indentation being averaged over the four radial traces); the mean and standard deviation over all indentations gives $K_c/\chi_r = 12.5 \pm 1.8$ MPa m$^{1/2}$. A detailed analysis of the elastic–plastic parameter in Equation 1 yields the relation $\chi_r = 0.014(E/H)^{1/2}$, where E and H are the Young's modulus and hardness (here defined as $P/2a^2$ for the Vickers geometry in Fig. 1), and the numerical constant is obtained by calibration with glass as a standard material (random error $< 10\%$) [12]. Thus for silicon, taking $E = 168$ GPa [25] and $H = 9.0$ GPa; $K_c = 0.76 \pm 0.19$ MPa m$^{1/2}$ is obtained as an

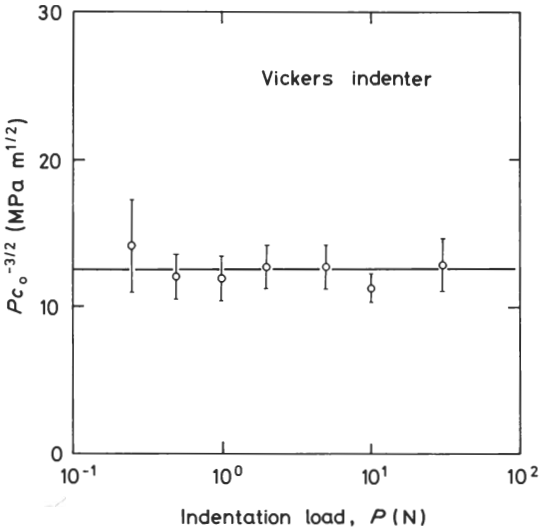

Figure 2 Plot of $P/c_0^{3/2}$ against P for silicon. Each data point is the mean and standard deviation of 7 indentations.

estimate of the toughness. This compares with fracture mechanics determinations by other workers [25–28], whose quoted values, corresponding to a variety of techniques and crystallographic planes, all fall within the range 0.5 to 1.0 MPa m$^{1/2}$.

3. Mechanics of failure from the radial crack system

Now the response of the radial crack system to a post-indentation tensile stress is considered. Detailed observations in glass [11] show that the applied tensile field is augmented by the residual field in such a way that the crack undergoes a precursor stage of stable expansion prior to reaching a failure configuration. The corresponding failure stress is significantly less (typically by ≈ 30 to 40%) than would be expected from the conventional theory of strength. It is of considerable interest to investigate whether this effect extends to silicon; for, if it does, any contact-induced flaw becomes a more likely source of premature breakdown in a component.

For this purpose a series of strength tests was run on sample bars cut from the (1 1 1) silicon slices; again, no attempt was made to orient the bars in any specific crystallographic direction along their length or width. Each bar (measuring 25 mm × 3 mm × 1 mm) was indented at the centre of a major face, at a load of $P = 30$ N, with the radial cracks aligned parallel to the edges. A simple cylindrical-support arrangement was contrived to stress the bars in three-point bending (span 10 mm), with the indentation site in the region of maximum tension. The bending force was delivered via a motor-driven double screw, and was simultaneously monitored by an instrumented proving ring [29]; simple-beam theory was then used to evaluate the corresponding bending stress. The entire stressing system was mounted onto the stage of an inverted microscope, so that the progress of the critical radial crack could be followed *in situ*. All testing was carried out in air. As with the preceding indentation observations, no evidence of any chemically-enhanced slow crack growth was found: e.g. bars loaded to within 99% of the failure stress showed no detectable extension over 5 min hold time (which, in conjunction with an estimated limit of ≈ 5 μm in resolution of the crack-tip location, corresponds to a velocity of $\lesssim 10^{-8}$ m sec^{-1} at $K = 0.99K_c$).

The radial crack growth to failure is plotted in Fig. 3 as applied tensile stress σ_a against crack size c (averaged over the two radial traces which constitute the critical crack, i.e. that crack perpendicular to the stress axis), for four bend specimens. In each case the existence of a precursor stage of extension is apparent, demonstrating the influence of the residual field. However, this extension does

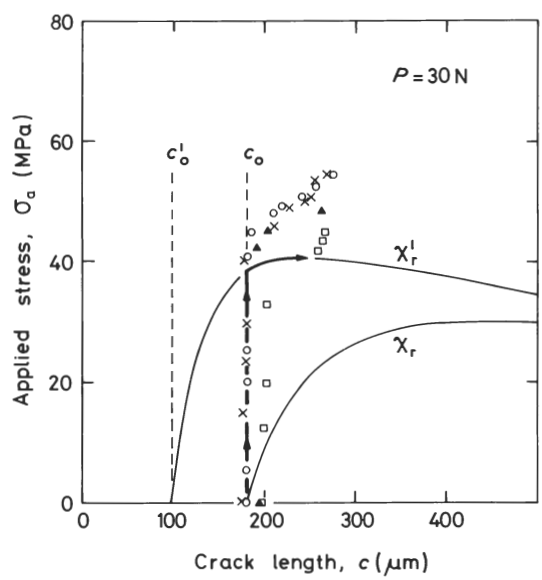

Figure 3 Radial crack growth in bend tests on pre-indented silicon bars (each symbol represents an individual bar). Curves are plots of Equation 4 corresponding to unrelaxed (χ_r) and relaxed (χ_r') residual fields, with arrowed lines designating the appropriate crack path to failure.

not begin until the applied stress reaches a fraction, somewhat more than one-half, of the critical level. Thus, at initial stressing the crack system is not, as implied in the derivation of Equation 2, in an equilibrium configuration; some relief process must operate to reduce K_r in Equation 1 below K_c between formation of the radials and application of the subsequent bending stresses. In glass, such relief is achieved effectively by moisture-assisted post-indentation crack expansion beyond c_0 [10, 11] (typically, K_r/K_c falls below 0.5 after less than 1 h exposure to air). But it has already been shown that slow crack growth effects are negligible in silicon, so an alternative explanation must be sought here. We are accordingly led to suggest that the intensity of the residual driving force, as characterized by the parameter χ_r in Equation 1, might be diminished by relaxation of the elastic constraint about the central deformation zone due to the incidence of lateral cracking. This explanation would be consistent with the relatively strong tendency to chipping previously noted in Section 1; in this connection, Petrovic *et al.* [30] have demonstrated that controlled abrasion of the indented surface (sufficient to remove a thin layer containing the lateral cracks and the central deformation zone, but without significantly reducing the size of the radial cracks) eliminates the residual stress field altogether. It may be noted that since development of the radial component precedes that of the lateral component in the crack evolution during the contact cycle, the value of χ_r appropriate to Equation 2 is not subject to such modification.

To investigate this interpretation quantitatively we begin with the stress intensity factor for radial cracks in tensile loading [11, 14],

$$K = K_r + K_a = \chi_r' P/c^{\frac{3}{2}} + \sigma_a(\pi\Omega c)^{\frac{1}{2}} \quad (c \geqslant c_0). \tag{3}$$

K_r follows directly from Equation 1, but with a "relaxed" elastic–plastic constant χ_r' replacing χ_r; K_a is the standard form for a uniform stress field, with Ω a geometrical constant. For equilibrium growth, $K = K_c$, Equation 3 may be solved explicitly for the functional dependence of applied stress on crack size,

$$\sigma_a = [K_c/(\pi\Omega c)^{\frac{1}{2}}](1 - \chi_r' P/K_c c^{\frac{3}{2}}). \tag{4}$$

An evaluation of the term in Ω is most conveniently obtained via strength tests on control specimens surface abraded to remove residual contact stresses, in which case failure occurs spontaneously (i.e. without precursor stable growth) from the indentation flaws at critical stressing; the results from 10 such tests over the contact load range $P = 10$ to 30 N, in conjunction with the insertions $\chi_r = 0$ and $\sigma_a = \sigma_0$ (residual-stress-free strength) at $c = c_0$ in Equation 4, gives $\sigma_0 c_0^{1/2} = 0.85 \pm 0.06$ MPa m$^{1/2} = K_c/(\pi\Omega)^{1/2}$. Now if in accordance with this "calibration" Equation 4 is plotted for $P = 30$ N using the value of K_c/χ_r obtained earlier from the indentation relation Equation 2 (i.e. with $\chi_r'/\chi_r = 1$) the lower curve in Fig. 3 is obtained, corresponding to a (true) initial crack size $c_0 = 180 \pm 18\,\mu$m. Even allowing for the considerable scatter in the experimental data, this curve is clearly not representative of the observed crack evolution. On the other hand, if due allowance is made for residual-field relaxation (i.e. a parametric adjustment is made in the range $\chi_r'/\chi_r < 1$) the curve calculated from Equation 4 undergoes a shift toward higher strength, with attendant truncated stable growth, as required; the upper curve in Fig. 3 is the computed function for $\chi_r'/\chi_r = 0.4$, corresponding to an (apparent) initial crack size $c_0' = 98\,\mu$m. The newly predicted crack path, indicated by the arrowed lines in the plot, provides a more reasonable (if not ideal) fit to the data.

A final series of strength tests was run on specimens indented over a range of loads to examine the effect of flaw severity in the failure mechanics. The results in Fig. 4 show a systematic decline in strength with increasing load, in a manner characteristic of sharp indenters [14, 31]. Degradation occurs without any apparent discontinuity in the data down to the low-load cutoff (shaded band) where pre-existing flaws control the strength, consistent with a threshold load < 0.1 N for radial crack initiation [23]. The straight line in the figure is the predicted strength degradation characteristic, obtained by maximizing the applied-stress–crack-size function in Equation 4 thus [11],

$$\sigma = \sigma_a(\mathrm{d}\sigma_a/\mathrm{d}c = 0) = \{(3/4^{\frac{4}{3}})\,[K_c/\chi_r']^{\frac{1}{3}}[K_c/(\pi\Omega)^{\frac{1}{2}}]\}/P^{\frac{1}{2}}, \tag{5}$$

with the square-bracket parameters the same as used to compute the modified crack path in Fig. 3. There appears to be a slight tendency for the data points at lower loads to fall below the plotted

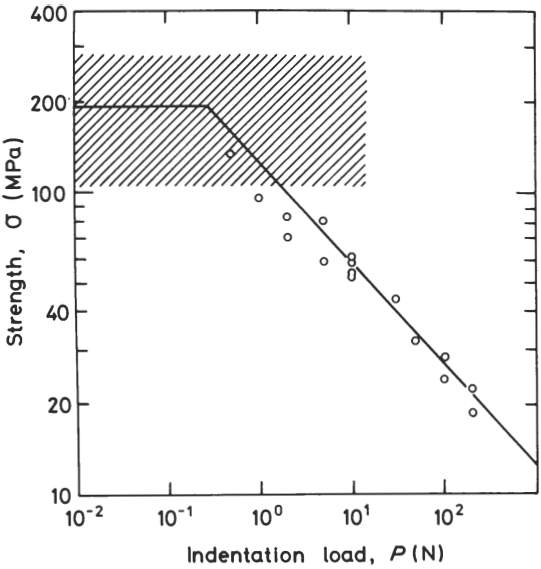

Figure 4 Failure stress of silicon bars as a function of indentation load. Cut-off strength level in low-load region (shaded band) represents the mean and standard deviation of 7 specimens which failed from pre-existing flaws.

line, suggesting that the degree of residual-stress relaxation might be somewhat less in this region; in this context it may be recalled that the prevalence of surface chipping does in fact tend to increase with the severity of contact.

4. Discussion

The analysis presented in this study provides a quantitative basis for predicting the strength of silicon components as a function of indentation history. In particular, silicon is characterized as a material of extreme brittleness, susceptible to severe loss of mechanical integrity from ostensibly minute contact events. The relevance of this work to the scribing process used in device fabrication, and to spurious particle impact in service environments, has already been mentioned: what the indentation–strength approach offers is a means of investigating such phenomena in a systematic and economic way, without the need to resort to statistically-based descriptions of strength.

From a more fundamental viewpoint, the indentation damage pattern may be expected to reflect on the micromechanics of naturally occurring flaws. Silicon single crystals can be grown to a high degree of perfection, free of any internal defects which might ordinarily constitute a potential source of fracture initiation; flaw genesis in this material is almost exclusively a function of surface-contact history.* Thus, in that the indentation test can be regarded as a representative model of the typical individual contact event encountered in practice, it may be concluded that silicon owes its flaw susceptibility to its deformation as well as to its fracture properties. Plasticity plays a vital role by creating the flaw nuclei and providing the primary driving force for extension of the ensuing cracks. There would appear to be a need for further microscopic study of this relatively unexplored area of fundamental strength analysis.

Although the radial crack system has been treated as the primary source of strength degradation in the above description, the co-existence of the lateral system needs always to be borne in mind. Quite apart from their influence in relaxing the residual driving force parameter χ_r (Section 3), the lateral cracks may, under certain circumstances, become the dominant flaws in a component. Such would be the case in diamond scribing, where the downward penetrating, linear median cracks are eliminated in the subsequent material-separation operation, leaving the laterals as prospective starting points for edge failure (a phenomenon of much concern in the glass industry [32]). Strength-testing procedures used in the evaluation of brittle components should therefore be designed to allow for this possibility, as is the case, for instance, with the four-point-twist test piece used by Chen [2].

Acknowledgements

The authors wish to acknowledge stimulating discussions with M. V. Swain, particularly on the role of lateral fracture in strength degradation. Funding for the project was provided by the Australian Research Grants Committee.

References

1. B. R. LAWN and D. B. MARSHALL, *J. Amer. Ceram. Soc.* 62 (1979) 347.
2. C. P. CHEN, "Fracture Strength of Silicon Solar Cells" (Jet Propulsion Laboratory Report 79-102, Pasadena, 1979).
3. A. MISRA and I. FINNIE, *J. Mater. Sci.* 14 (1979) 2567.
4. D. HANEMAN, W. D. ROOTS and J. T. P. GRANT,

*Although the "contact" need not be mechanical in nature, e.g. as in "laser scribing" [21].

J. Appl. Phys. **38** (1967) 2203.
5. B. P. LEMKE and D. HANEMAN, *Phys. Rev. B* **17** (1978) 1893.
6. B. R. LAWN and M. V. SWAIN, *J. Mater. Sci.* **10** (1975) 113.
7. B. R. LAWN and T. R. WILSHAW, *ibid.* **10** (1975) 1049.
8. B. R. LAWN and E. R. FULLER, *ibid.* **10** (1975) 2016.
9. A. G. EVANS and T. R. WILSHAW, *Acta. Met.* **24** (1976) 939.
10. D. B. MARSHALL and B. R. LAWN, *J. Mater. Sci.* **14** (1979) 2001.
11. D. B. MARSHALL, B. R. LAWN and P. CHANTIKUL, *ibid.* **14** (1979) 2225.
12. B. R. LAWN, A. G. EVANS and D. B. MARSHALL, *J. Amer. Ceram. Soc.* **63** (1980) 574.
13. B. J. HOCKEY, S. M. WIEDERHORN and H. JOHNSON, in "Fracture Mechanics of Ceramics", edited by R. C. Bradt, D. P. H. Hasselman and F. F. Lange (Plenum, New York, 1978) p. 379.
14. B. R. LAWN, D. B. MARSHALL, P. CHANTIKUL and G. R. ANSTIS, *J. Aust. Ceram. Soc.* **16** (1980) 4.
15. V. G. EREMENKO and V. I. NIKITENKO, *Phys. Stat. Sol. (a)* **14** (1972) 317.
16. M. J. HILL and D. J. ROWCLIFFE, *J. Mater. Sci.* **9** (1974) 1569.
17. P. HUMBLE and R. H. J. HANNINK, *Nature* **273** (1978) 37.
18. B. R. LAWN, B. J. HOCKEY and S. M. WIEDERHORN, *J. Mater. Sci.* **15** (1980) 1207.
19. K. E. PUTTICK and M. A. SHAHID, *Ind. Diamond Rev.* (July, 1977) 208.
20. A. S. T. BADRICK, F. ELDEGHAIDY, K. E. PUTTICK and M. A. SHAHID, *J. Phys. D: Appl. Phys.* **10** (1977) 195.
21. H. KOTAKE and S. TAKASU, *J. Mater. Sci.* **15** (1980) 895.
22. B. R. LAWN and A. G. EVANS, *ibid.* **12** (1977) 2195.
23. J. LANKFORD and D. L. DAVIDSON, *ibid.* **14** (1979) 1662.
24. B. R. LAWN, *J. Appl. Phys.* **39** (1968) 4828.
25. R. J. JACCODINE, *J. Electrochem. Soc.* **110** (1963) 524.
26. J. J. GILMAN, *J. Appl. Phys.* **31** (1960) 2208.
27. C. ST. JOHN, *Phil. Mag.* **32** (1975) 1193.
28. C. P. CHEN and M. H. LEIPOLD, *Amer. Ceram. Soc. Bull.* **59** (1980) 469.
29. V. R. HOWES, *Glass Tech.* **15** (1974) 148.
30. J. J. PETROVIC, R. A. DIRKS, L. A. JACOBSON and M. G. MENDIRATTA, *J. Amer. Ceram. Soc.* **59** (1976) 177.
31. B. R. LAWN and D. B. MARSHALL, in "Fracture Mechanics of Ceramics", edited by R. C. Bradt, D. P. H. Hasselman and F. F. Lange (Plenum, New York, 1978) p. 205.
32. M. V. SWAIN, unpublished work (1980).

Received 27 October and accepted 2 December 1980.